

# Comparison BIPM.RI(I)-K8 of high dose-rate $^{192}\text{Ir}$ brachytherapy standards for reference air kerma rate of the PTB and the BIPM

C Kessler<sup>1</sup>, R Behrens<sup>2</sup>, A Kasper<sup>2</sup>, F Grote<sup>2</sup>

<sup>1</sup>Bureau International des Poids et Mesures, F-92312 Sèvres Cedex, France

<sup>2</sup>Physikalisch-Technische Bundesanstalt, D-38116 Braunschweig, Germany

## Abstract

An indirect comparison of the standards for reference air kerma rate for  $^{192}\text{Ir}$  high dose rate (HDR) brachytherapy sources of the Physikalisch-Technische Bundesanstalt (PTB), Germany, and of the Bureau International des Poids et Mesures (BIPM) was carried out at the PTB in May 2023. The comparison result, based on the calibration coefficients for a transfer standard and expressed as a ratio of the PTB and the BIPM standards for reference air kerma rate, is 1.0022 with a combined standard uncertainty of 0.0101.

## 1. Introduction

The Brachytherapy Standards Working Group (BSWG(I)), created under the recommendation made by the Consultative Committee for Ionizing Radiation CCRI(I), proposed at their meeting of November 2005 to start a comparison of primary standards for reference air kerma rate (RAKR) of  $^{192}\text{Ir}$ . To meet the needs of the National Metrology Institutes (NMIs), a new ongoing key comparison was registered in the BIPM key comparison data base (KCDB 2023) under the reference BIPM.RI(I)-K8. As no primary facility for brachytherapy is available at the BIPM, the measurements take place at the NMI. The BIPM results are based on measurements using transfer standards, an NE 2571 thimble-type transfer ionization chamber and a well-type ionization chamber.

The Physikalisch-Technische Bundesanstalt (PTB) took part in the comparison in May 2023 to update the previous comparison result of 2011 (Kessler *et al.* 2015) published in the KCDB. The comparison was carried out after the implementation of the recommendations of ICRU Report 90 (ICRU 2016) at both laboratories.

The previous comparison was done using the thimble chamber and the well-type chamber. As the PTB provides traceability for HDR  $^{192}\text{Ir}$  sources calibrating only well-type chambers, the present comparison was run using only the well-type chamber and the result is given in terms of the ratio of the calibration coefficient determined at the PTB and the reference value used by the BIPM. The BIPM reference value is the mean of the calibration coefficients determined by the BIPM during the comparisons with the NMIs that have participated calibrating the thimble chamber during the period 2009-2014 (VSL, NPL, PTB and NRC).

The long-term stability of the well chamber is established by measurements at the BIPM using a  $^{137}\text{Cs}$  source.

The comparison result, approved by the CCRI, is analysed and presented in terms of degrees of equivalence for entry in the BIPM key comparison database.

## 2. Characteristics of the transfer instrument

The transfer instrument, belonging to the BIPM, used to undertake the comparison, was a Standard Imaging HDR 1000 Plus well chamber. The main characteristics of the transfer instrument are listed in Table 1.

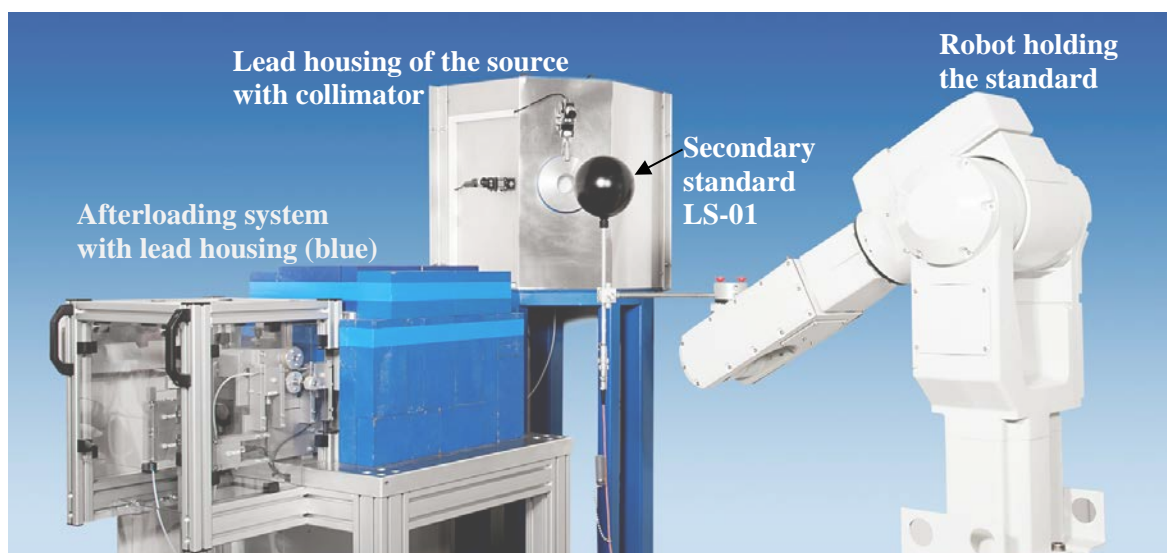
**Table 1. Characteristics of the BIPM transfer chamber**

| Characteristic/Nominal values |  | Standard Imaging |              |
|-------------------------------|--|------------------|--------------|
|                               |  | HDR 1000 Plus    | Insert 70010 |
| Dimensions                    | Inner diameter / mm                      | 102              | 35           |
|                               | Cavity length / mm                       | 156              | 121          |
|                               | Bottom of insert to reference point / mm | 50 (sweet-spot)  |              |
| Air cavity                    | Volume / cm <sup>3</sup>                 | 245              |              |
| Voltage applied               | Polarity to outer electrode / V          | + 300            |              |

## 3. Determination of the PTB reference value

For nearly three decades, PTB has been offering the calibration of <sup>192</sup>Ir and <sup>60</sup>Co high dose rate (HDR) brachytherapy sources in terms of RAKR. The PTB also offers the calibration of well-type chambers for both radionuclides. The RAKR is determined from measurements using a reference ionization chamber in a collimated radiation field, achieved by positioning the source in the center of a lead chamber of 30 cm x 30 cm x 40 cm, 5 cm wall thickness and collimators made of DensiMet® (alloy of approximately 92 % tungsten, 4 % nickel and 4 % iron with a density of nearly 18 g/cm<sup>3</sup>) with a diameter of either 5.5 cm or 11 cm; a robot is used to position the reference ionization chamber on the central axis of the radiation field defined by the collimator (Fig. 1).

**Figure 1. Set-up for the calibration of HDR-brachytherapy sources in a collimated field**



A secondary standard LS-01 ionization chamber is used to determine the RAKR. To assess its position with respect to the center of the radiation source with an accuracy better than 0.1 mm, measurements at five different distances from 800 mm to 1600 mm in steps of 200 mm are

made. After applying appropriate corrections for scattering and attenuation in air, the inverse square law is used to calculate the source position.

The correction factors associated with the scattering and the attenuation in air were determined by measurements applying the shadow shield method, supported by Monte Carlo calculations (Selbach and Büermann 2004).

Until 2022, the LS-01 calibration coefficient for  $^{192}\text{Ir}$  was determined from the energy response of the chamber from 20 kV to 300 kV,  $^{137}\text{Cs}$  and  $^{60}\text{Co}$  radiation beams and using the energy spectrum of the  $^{192}\text{Ir}$  source. To determine the energy dependence, the chamber was calibrated in the mentioned energy range against the x-ray primary free air chambers PK 100 and PK 400 and gamma-ray primary cavity standard HRK-3. The calibration coefficients were weighted with the line spectrum of the  $^{192}\text{Ir}$  source to obtain the corresponding  $^{192}\text{Ir}$  calibration coefficient for the LS-01 (Selbach and Büermann 2004 and Kessler *et al.* 2015). Repeat calibrations were done every two years; the stability of the chamber was determined to be 1 part in  $10^3$  for the gamma-ray beams and about 1 part in  $10^2$  for the low-energy range of x-ray beams.

In 2018, the PTB implemented the recommendations of the ICRU 90 report, resulting in a decrease of the  $^{192}\text{Ir}$  calibration coefficient of 3.4 parts in  $10^3$ . The decrease factor of 0.9966 was obtained from interpolation considering the change of the N-300 x-ray quality (300 kV) and  $^{137}\text{Cs}$ , for the 400 keV mean energy of  $^{192}\text{Ir}$  (Büermann 2018).

In 2023, the PTB adopted new standards, namely, two PTW graphite-walled, spherical, air-filled cavity ionization chambers PS-10 and PS-50, fully characterized to be considered as primary cavity chamber standards for  $^{60}\text{Co}$ ,  $^{137}\text{Cs}$  and  $^{192}\text{Ir}$  sources: the cavity volume was measured and correction factors for the chamber were derived from both measurements and Monte Carlo simulations. The description of the standards can be found in Pojtinger and Büermann (2021). The PS-50 primary standard was used to determine the RAKR reference value for  $^{192}\text{Ir}$  and to recalibrate the LS-01 chamber. The direct calibration coefficient of the LS-01 determined against the PS-50 primary standard was found to be lower than the interpolated coefficient by 8.3 parts in  $10^3$  (i.e., a decrease factor of 0.9917).

In summary, the overall change implemented at the PTB results in a reduction of the 2011 RAKR reference value of 1.17 parts in  $10^2$ . Further details regarding the two changes can be found at the PTB website (Behrens and Pojtinger 2023).

The main characteristics of the new primary standards and the LS-01 are listed in Table 2.

**Table 2. Characteristics of the PTB primary and secondary standards \***

| Characteristic/Nominal values                                  |                            | PS-10  | PS-50  | LS-01 |
|--|----------------------------|--------|--------|-------|
| Dimensions   | Inner diameter / mm        | 27     | 46     | 134   |
|  | Wall thickness / mm        | 3.5    | 3.5    | 3     |
| Electrode  | Diameter / mm              | 3      | 3      | 50    |
| Volume   | Air cavity / $\text{cm}^3$ | 10.003 | 49.902 | 1000  |
| Graphite wall density / $\text{g cm}^{-3}$                     |                            | 1.839  | 1.821  | ---   |
| Polyoxymethylene (POM) wall density / $\text{g cm}^{-3}$       |                            | ---    | ---    | 1.51  |
| Potential of HV electrode with respect to collecting electrode |                            | +500   | +500   | +400  |

\* Data obtained from Pojtinger and Büermann 2021 and PTW catalogue 2023

The RAKR is determined using the expression

$$\dot{K}_R = k_{\text{aniso}} \cdot \overline{\dot{K}_{R,i}} \quad (1)$$

where

$\dot{K}_R$  is the RAKR at the chosen reference time of the comparison,

$k_{\text{aniso}}$  is the correction factor for the source anisotropy in radial direction, and

$\overline{\dot{K}_{R,i}}$  is the mean value of the RAKR  $\dot{K}_{R,i}$  determined at 5 distances  $i$  ( $i = 1$  to 5) from 800 mm to 1600 mm in steps of 200 mm:

$$\dot{K}_{R,i} = N \cdot (I_i - I_{\text{leak}}) \cdot k_{\text{dist}_i} \cdot k_{\rho,\text{air}_i} \cdot (d_i - d_{\text{off}})^2 \cdot k_{\text{sat}} \cdot k_{\text{dec}_i} \quad (2)$$

where

$N$  is the calibration coefficient of the LS-01 chamber,

$I_i$  is the ionization current measured using the LS-01 at distance  $i$ ,

$I_{\text{leak}}$  is the leakage current,

$k_{\text{dist}_i}$  is the correction factor for scattering and attenuation at distance  $i$ ,

$k_{\rho,\text{air}_i}$  is the air temperature and pressure correction factor at distance  $i$ ,

$d_i$  is the value of the source-detector distance at distance  $i$ ,

$d_{\text{off}}$  is the offset of the detector distance (determined from inverse square law),

$k_{\text{sat}}$  is the saturation correction factor and

$k_{\text{dec}_i}$  is the source decay correction factor.

The values used for the physical constants, the correction factors entering in the determination of the RAKR at the reference distance of 1 m and the associated uncertainties are given in Table 3.

The first five lines of the table give the values of the RAKR,  $\dot{K}_{R,i}$ , and the associated uncertainties at each of the five distances. The final RAKR,  $\dot{K}_R$ , in the last line of the table results from averaging the five (correlated) RAKR values,  $\dot{K}_{R,i}$ , corrected by the factor  $k_{\text{aniso}}$ , the source anisotropy in radial direction. The relative combined uncertainty, removing correlations, is 1.21 parts in  $10^2$ .

**Table 3. Physical constants and correction factors with their relative standard uncertainties of the PTB LS-01 standard for the  $^{192}\text{Ir}$  radiation beam**

| Quantity              | Value                     | Standard Uncertainty     |          | Uncertainty contribution* |
|-----------------------|---------------------------|--------------------------|----------|---------------------------|
|                       |                           | absolute                 | relative |                           |
| $RAKR_{800}$          | 13.992 (mGy/h)            | 0.158 (mGy/h)            | 1.13 %   |                           |
| $RAKR_{1000}$         | 13.987 (mGy/h)            | 0.158 (mGy/h)            | 1.13 %   |                           |
| $RAKR_{1200}$         | 13.990 (mGy/h)            | 0.158 (mGy/h)            | 1.14 %   |                           |
| $RAKR_{1400}$         | 13.993 (mGy/h)            | 0.157 (mGy/h)            | 1.12 %   |                           |
| $RAKR_{1600}$         | 13.984 (mGy/h)            | 0.157 (mGy/h)            | 1.12 %   |                           |
| $k_{\text{aniso}}$    | 1.0000                    | 0.0029                   | 0.29 %   | 9.0 %                     |
| $N$                   | 24956 Gy/C                | 212 Gy/C                 | 0.85 %   | 77.9 %                    |
| $I_{\text{leak}}$     | $0.014 \cdot 10^{-12}$ A  | $0.010 \cdot 10^{-12}$ A | 71 %     | 0.0 %                     |
| $d_{\text{off}}$      | 3.9 mm                    | 0.4 mm                   | 10 %     | 0.5 %                     |
| $k_{\text{dec}}$      | 0.34238                   | 0.00007                  | 0.019 %  | 0.0 %                     |
| $k_{\text{sat}}$      | 1.000                     | 0.001                    | 0.10 %   | 1.1 %                     |
| $I_{800}$             | $711.60 \cdot 10^{-12}$ A | $0.14 \cdot 10^{-12}$ A  | 0.020 %  | 0.0 %                     |
| $k_{\text{dist}800}$  | 1.009                     | 0.007                    | 0.70 %   | 2.1 %                     |
| $k_{\rho 800}$        | 1.000                     | 0.002                    | 0.20 %   | 0.2 %                     |
| $d_{800}$             | 800.02 mm                 | 0.10 mm                  | 0.012 %  | 0.0 %                     |
| $I_{1000}$            | $453.60 \cdot 10^{-12}$ A | $0.09 \cdot 10^{-12}$ A  | 0.020 %  | 0.0 %                     |
| $k_{\text{dist}1000}$ | 1.010                     | 0.007                    | 0.70 %   | 2.1 %                     |
| $k_{\rho 1000}$       | 1.000                     | 0.002                    | 0.20 %   | 0.2 %                     |
| $d_{1000}$            | 1000.01 mm                | 0.10 mm                  | 0.010 %  | 0.0 %                     |
| $I_{1200}$            | $314.10 \cdot 10^{-12}$ A | $0.06 \cdot 10^{-12}$ A  | 0.020 %  | 0.0 %                     |
| $k_{\text{dist}1200}$ | 1.012                     | 0.007                    | 0.70 %   | 2.1 %                     |
| $k_{\rho 1200}$       | 1.000                     | 0.002                    | 0.20 %   | 0.2 %                     |
| $d_{1200}$            | $1200.01 \cdot 10^3$ mm   | 0.10 mm                  | 0.008 %  | 0.0 %                     |
| $I_{1400}$            | $230.20 \cdot 10^{-12}$ A | $0.05 \cdot 10^{-12}$ A  | 0.020 %  | 0.0 %                     |
| $k_{\text{dist}1400}$ | 1.014                     | 0.007                    | 0.70 %   | 2.1 %                     |
| $k_{\rho 1400}$       | 1.000                     | 0.002                    | 0.20 %   | 0.2 %                     |
| $d_{1400}$            | $1400.00 \cdot 10^3$ mm   | 0.10 mm                  | 0.007 %  | 0.0 %                     |
| $I_{1600}$            | $175.70 \cdot 10^{-12}$ A | $0.04 \cdot 10^{-12}$ A  | 0.020 %  | 0.0 %                     |
| $k_{\text{dist}1600}$ | 1.016                     | 0.007                    | 0.70 %   | 2.1 %                     |
| $k_{\rho 1600}$       | 1.000                     | 0.002                    | 0.20 %   | 0.2 %                     |
| $d_{1600}$            | $1600.00 \cdot 10^3$ mm   | 0.10 mm                  | 0.006 %  | 0.0 %                     |
| $RAKR$                | 13.989 (mGy/h)            | 0.135 (mGy/h)            | 0.97 %   | 100 %                     |

(\*) Uncertainty contribution:  $(c_i \cdot u_i)^2 / \sum \{(c_i \cdot u_i)^2\}$  with the sensitivity coefficient  $c_i$  and the standard uncertainty  $u_i$  of the input quantity  $i$ . The sensitivity coefficient  $c_i$  is given by the partial derivative of the output quantity ( $RAKR$ ) with respect to the input quantity  $i$ .

The main characteristics of the HDR  $^{192}\text{Ir}$  source used at the PTB are listed in Table 4.

**Table 4.** Characteristics of the PTB  $^{192}\text{Ir}$  source

|                                      |                                    |
|--------------------------------------|------------------------------------|
| After-loader unit                    | custom made afterloading system    |
| Manufacturer of source               | Curium Netherlands B.V.            |
| Source type                          | MICROSELECTRON V2                  |
| Source Model Designation             | 105.002                            |
| Source serial number                 | D36Q1473                           |
| Estimated content activity of source | 411.3 GBq at 2023-01-04, 12:28 CET |
| Capsule dimensions                   | 0.9 mm diameter, 4.5 mm length     |
| Capsule material                     | Stainless steel, AISI 316L         |
| Source pellet dimensions             | 0.6 mm diameter, 3.5 mm length     |

#### 4. Determination of the BIPM reference value

The BIPM does not possess an  $^{192}\text{Ir}$  source. The reference value for the well-type HDR 1000 Plus ionization chamber is based on measurements made using the  $^{192}\text{Ir}$  sources of the four laboratories participating in the BIPM.RI(I)-K8 comparison during the period 2009-2014. The stability of the well chamber is monitored using a sealed source of  $^{137}\text{Cs}$ . The long-term reproducibility of the chamber established using this source is less than 1 part in  $10^3$  in relative value.

To derive a reference value for the well chamber, the BIPM determines its calibration coefficient at each NMI that participates in this on-going key comparison through calibration of the thimble-type NE 2571 ionization chamber. Using the NMI  $^{192}\text{Ir}$  source, the calibration coefficient for the well-type chamber  $N_{K,\text{BIPM}}^w$  is evaluated as

$$N_{K,\text{BIPM}}^w = \frac{\dot{K}_{R,\text{BIPM}}}{I_w} \quad (3)$$

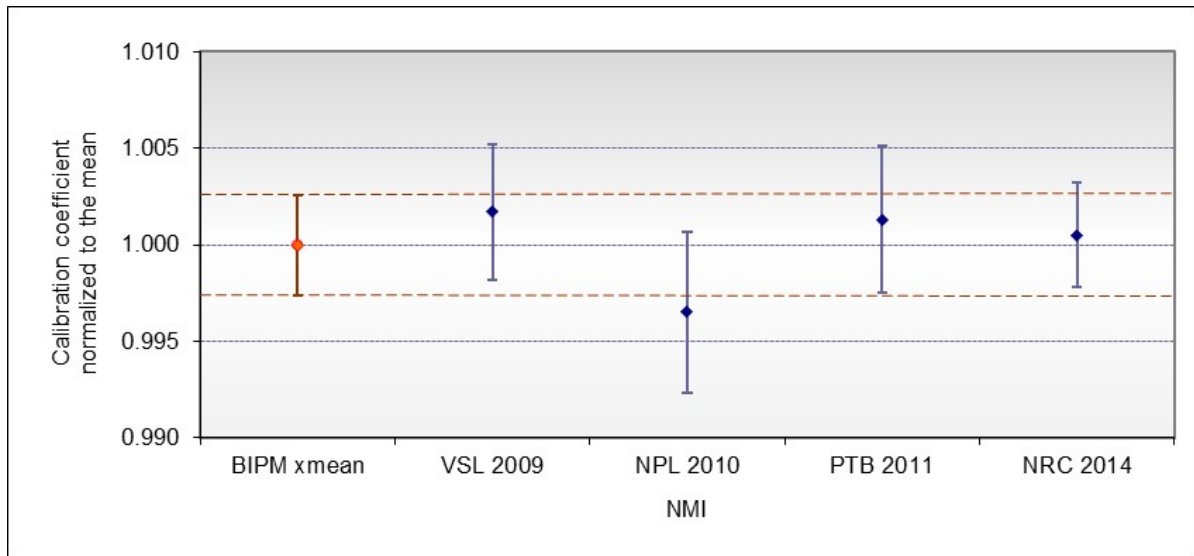
where  $\dot{K}_{R,\text{BIPM}}$  is the RAKR for the NMI source evaluated from the current determined by the NMI using the BIPM NE 2571 thimble chamber  $I^{\text{th}}$  and its calibration coefficient  $N_{K,\text{BIPM}}^{\text{th}}$  determined by the BIPM ( $\dot{K}_{R,\text{BIPM}} = I^{\text{th}} N_{K,\text{BIPM}}^{\text{th}}$ ), as described in the protocol for this on-going key comparison<sup>a</sup>.

The well chamber current  $I_w$ , measured at the sweet-spot, is appropriately corrected to the reference conditions of measurements and normalized to the reference ambient conditions.

The mean of the well chamber calibration coefficients determined by the BIPM at each NMI that calibrated the NE 2571 chamber during the period 2009-2014 is taken as the reference value for the well chamber. To date, four NMIs (VSL, NPL, PTB and NRC) have participated in the BIPM.RI(I)-K8 comparison by calibrating the NE 2571 chamber (Alvarez *et al.* 2014a, Alvarez *et al.* 2014b, Kessler *et al.* 2015 and Kessler *et al.* 2014). The normalized calibration coefficients determined by the BIPM at these NMIs are shown in Figure 2. The standard deviation of the mean is 1.2 parts in  $10^3$ ; the evaluation of the standard uncertainty is explained in Section 7 and is represented in the graph by the dotted line.

<sup>a</sup> The value  $N_{K,\text{BIPM}}^{\text{th}}$  for  $^{192}\text{Ir}$  is calculated from the calibration coefficient determined at the BIPM in the  $^{60}\text{Co}$  reference beam and a correction factor that accounts for the energy dependence of the chamber; this factor was calculated using a Monte Carlo code (Mainegra-Hing and Rogers 2006) to simulate the chamber response from 100 keV to  $^{60}\text{Co}$  beams.

**Figure 2. Normalized BIPM calibration coefficient for the well chamber**



The uncertainty bars represent one standard uncertainty

## 5. Comparison measurements at the PTB

The HDR 1000 Plus well chamber, together with its electrometer and probes for temperature, pressure and humidity, is used as a transfer system to determine a comparison result for those NMIs that do not provide calibrations of thimble-type ionization chambers. The ionization current of the well chamber was measured at the PTB and the BIPM calibration coefficient was derived from these measurements and the PTB determination of RAKR, as described in Section 3.

The essential details of the current measurements are reproduced here.

### *Sweet-spot*

At the PTB, measurements at seven dwell positions for the  $^{192}\text{Ir}$  source with steps of 2 mm were done to determine the sweet-spot of the well chamber.

### *Charge and leakage measurements*

At the sweet spot, four series of 20 charge measurements over 60 s each were made, the source being retracted to the afterloader and repositioned at the sweet-spot between each series. Measurements were also made at  $\pm 1$  mm and  $\pm 2$  mm of the sweet-spot to confirm the position of the source. The standard deviation of the mean value of the four series was estimated to be 5 parts in  $10^4$ .

Measurements were corrected for leakage, which was measured before and after each series. This correction was, in relative value, less than 1 part in  $10^3$ .

### *Ambient conditions*

The measurements are normalized to 293.15 K and 101.325 kPa. No humidity correction is applied.

### *Decay correction*

The measurements are corrected for the decay of the source to the reference date of 2023-05-10, 12:00 UTC. The half-life for  $^{192}\text{Ir}$  is 73.827 days with  $u_c = 0.013$  days, taken from Bé *et al.* (1999).

## 6. Results of the comparison

The individual calibration coefficients of the well chamber will not be disclosed as this transfer chamber will be calibrated by other NMIs participating in this ongoing comparison.

The calibration coefficient  $N_{K,PTB}^w$  for the PTB is determined as

$$N_{K,PTB}^w = \frac{\dot{K}_{R,PTB}}{I_w} \quad (4)$$

where  $\dot{K}_{R,PTB}$  is the PTB reference air kerma rate and  $I_w$  is the well chamber current.

As noted in Section 4, at the time of producing this report, four NMIs had participated in the BIPM.RI(I)-K8 comparison using the NE 2571 chamber (VSL, NPL, PTB and NRC). Taking the mean,  $\bar{N}_{K,BIPM}^w$ , of the four values determined by the BIPM at these NMIs, it is possible to evaluate the comparison result for the PTB expressed as

$$R_{K,PTB}^w = \frac{N_{K,PTB}^w}{\bar{N}_{K,BIPM}^w} \quad (5)$$

For the PTB, the comparison result  $R_K^w$  is 1.0022.

## 7. Uncertainties

As explained in Section 6, the BIPM calibration coefficient for the well chamber for  $^{192}\text{Ir}$  beams is the mean of the calibration coefficients obtained at each NMI. Table 5 summarizes the uncertainty  $u_i$  corresponding to each calibration and the uncertainty of the mean value  $u$ , taking correlation into account.

**Table 5. Relative standard uncertainty associated with the BIPM well chamber calibration at the NMIs**

| Relative standard uncertainty                             | $u_i$  |
|---|--------|
| $N_{K,BIPM}^w$ at the VSL (1st comparison 2009)           | 0.0035 |
| $N_{K,BIPM}^w$ at the NPL (1st comparison 2010)           | 0.0042 |
| $N_{K,BIPM}^w$ at the PTB (1st comparison 2011)           | 0.0038 |
| $N_{K,BIPM}^w$ at the NRC                                 | 0.0027 |
| $\bar{N}_{K,BIPM}^w$ <sup>(a)</sup> for $^{192}\text{Ir}$ | 0.0026 |

<sup>(a)</sup> Correlation between the four determinations has been taken into account

The relative standard uncertainties associated with the well-type chamber calibration at the PTB are listed in Table 6.



**Table 6. Relative standard uncertainties associated with the well chamber calibration at the PTB**

| Relative standard uncertainty                        | PTB      |          |
|--|----------|----------|
|  | $u_{iA}$ | $u_{iB}$ |
| <i><sup>192</sup>Ir air kerma determination</i>      |          |          |
| Reference air kerma rate $\dot{K}_R$                 | 0.0045   | 0.0086   |
| <i>Calibration of the well-type chamber</i>          |          |          |
| Ionization current measured with well chamber, $I_w$ | 0.0002   | 0.0002   |
| Temperature, pressure correction                     | ---      | 0.0001   |
| Short-term stability                                 | 0.0005   | ---      |
| $N_{K,PTB}^w$  | 0.0045   | 0.0086   |

From Tables 5 and 6, the combined standard uncertainty  $u_c$  for the comparison result  $R_{K,PTB}^w$  is 10.1 parts in  $10^3$ .

## 8. Discussions

Since 2019 and following the decision of the CCRI(I), the BIPM and the participating laboratories started to implement the recommendations of the ICRU 90. Some laboratories have also implemented some improvements to their standards, and the resulting changes adopted by the NMIs to update the comparison results are summarized in Table 7.

**Table 7. Comparison results updated with the changes implemented by the NMIs**

| Year of participation                  | NMI               | NMI change          | Comparison result pre-2019 | Updated comparison result |
|--|-------------------|---------------------|----------------------------|---------------------------|
|  | BIPM              | 0.9913              |                            |                           |
| 2009                                   | VSL <sup>a</sup>  | 0.9943              | 0.9873                     | 0.9903                    |
| 2010                                   | NPL <sup>a</sup>  | 1.0029              | 0.9989                     | 1.0106                    |
| 2011                                   | PTB <sup>a</sup>  | 0.9883 <sup>c</sup> | 1.0003                     | 0.9973                    |
| 2014                                   | NRC <sup>a</sup>  | 0.9955              | 0.9966                     | 1.0009                    |
| 2015                                   | NMIJ <sup>b</sup> | 0.9917              | 1.0036                     | 1.0040                    |
| New participation in the BIPM.RI(I)-K8 |                   |                     |                            | New comparison result     |
| 2022                                   | NPL <sup>b</sup>  |                     |                            | 1.0045                    |
| 2023                                   | PTB <sup>b</sup>  |                     |                            | 1.0022                    |

<sup>a</sup> results obtained using the thimble chamber

<sup>b</sup> results obtained using the well-type chamber

<sup>c</sup> Further details regarding the change can be found at the PTB website (Behrens and Pojtinger 2023)

## 9. Degrees of equivalence

For each NMI  $i$  having a comparison result  $R_{K,i}$  (denoted  $x_i$  in the KCDB) with combined standard uncertainty,  $u_i$ , the degree of equivalence with respect to the key comparison reference value is given by a pair of terms:

$$\text{the relative difference } D_i = (N_{K_R, \text{NMI } i} - N_{K_R, \text{BIPM}}) / N_{K_R, \text{BIPM}} = R_{K,i} - 1 \quad (6)$$

$$\text{and its expanded uncertainty } U_i = 2 u_i. \quad (7)$$

The results for  $D_i$  and  $U_i$ , are expressed in mGy/Gy. Table 8 gives the values for  $D_i$  and  $U_i$  for the NMIs that have participated to date, taken from the KCDB of the CIPM MRA (1999) and this report. These data are presented graphically in Figure 3.

**Table 8. Degrees of equivalence**

For each laboratory  $i$ , the degree of equivalence with respect to the key comparison reference value is the difference  $D_i$  and its expanded uncertainty  $U_i$ . Tables formatted as they appear in the BIPM key comparison database (KCDB 2023)

BIPM.RI(I)-K8

| Lab $i$        | $D_i$     | $U_i$ |
|----------------|-----------|-------|
|                | /(mGy/Gy) |       |
| a) <b>VSL</b>  | -9.7      | 12.0  |
| a) <b>NRC</b>  | 0.9       | 10.0  |
| b) <b>NMIJ</b> | 4.0       | 10.8  |
| b) <b>NPL</b>  | 4.5       | 8.6   |
| b) <b>PTB</b>  | 2.2       | 20.2  |

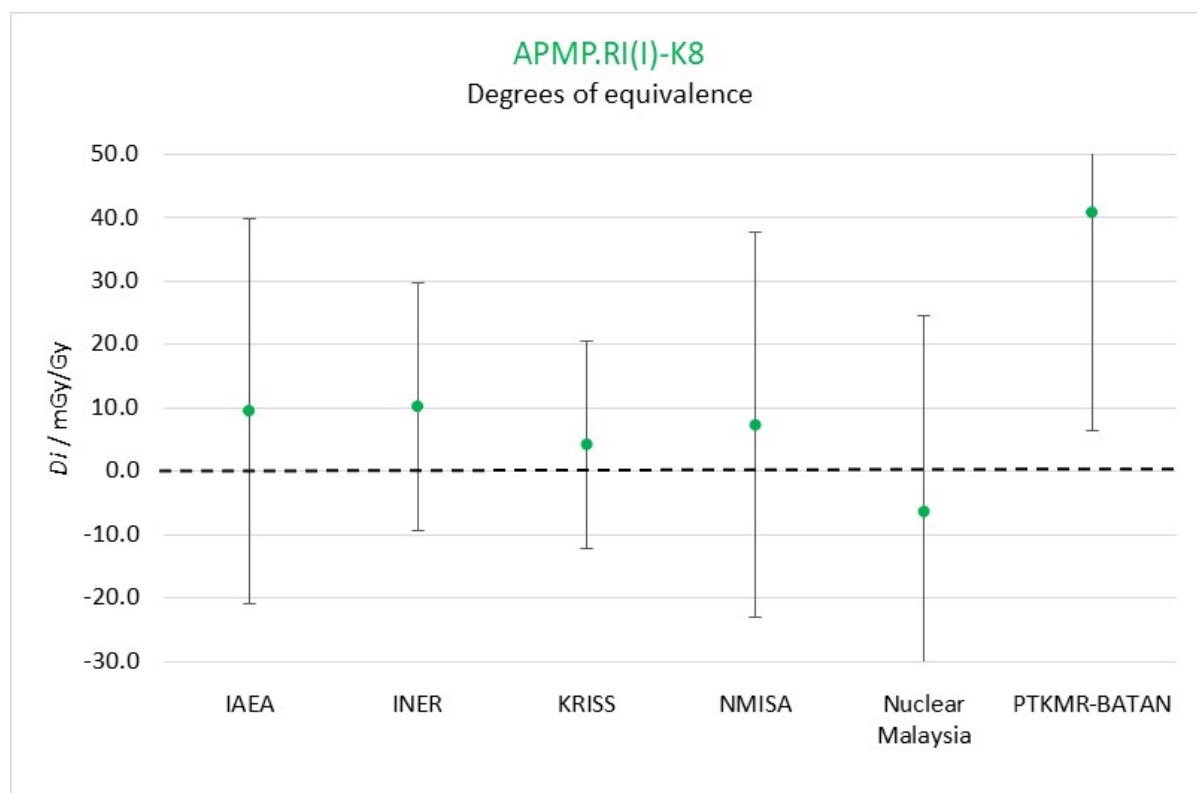
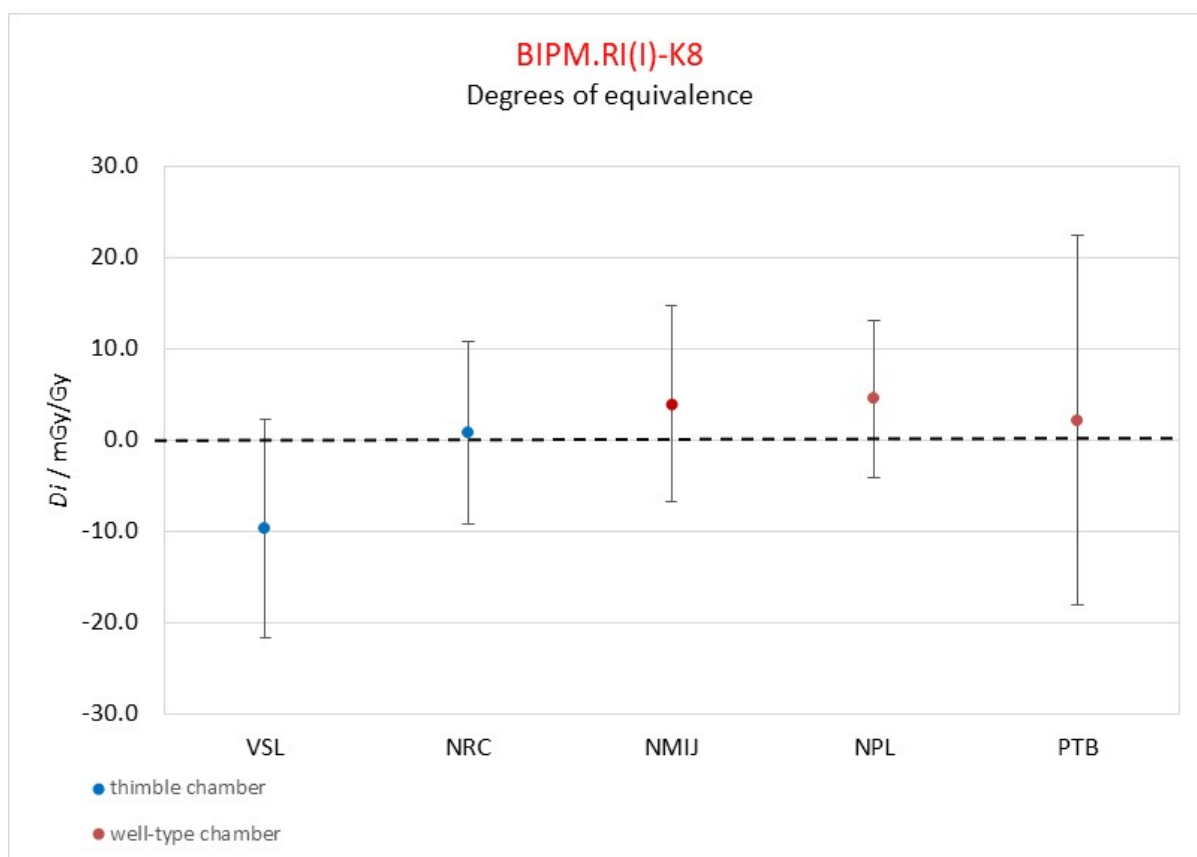
a) results obtained using a thimble-type chamber

b) results obtained using a well-type chamber

APMP.RI(I)-K8

| Lab $i$                 | $D_i$     | $U_i$ |
|-------------------------|-----------|-------|
|                         | /(mGy/Gy) |       |
| <b>IAEA</b>             | 9.4       | 30.4  |
| <b>INER</b>             | 10.1      | 19.6  |
| <b>KRISS</b>            | 4.2       | 16.4  |
| <b>NMISA</b>            | 7.3       | 30.4  |
| <b>Nuclear Malaysia</b> | -6.4      | 30.8  |
| <b>PTKMR-BATAN</b>      | 40.8      | 34.4  |

**Figure 3. Graph of degrees of equivalence with the KCRV**



## 9. Conclusion

The PTB standard for the reference air kerma rate for  $^{192}\text{Ir}$  gamma radiation compared with the BIPM reference value gives a comparison result of 1.0022 with a combined standard uncertainty  $u_c$  of 0.0101.

The previous comparison, done using the calibration coefficient of the thimble chamber, was 1.0003 (99). This result, updated with the changes implemented by the PTB and the BIPM, becomes 0.9973 (126), in agreement within the uncertainties with the present result.

The degrees of equivalence with the NPL, NRC, NMJJ and the VSL, so far the only four other participants in the BIPM.RI(I)-K8 comparison, are within the expanded uncertainty.

## References

- Alvarez J T, de Pooter J A, Andersen C, Aalbers A H L, Allisy-Roberts P J and Kessler C 2014a Comparison BIPM.RI(I)-K8 of high dose rate  $^{192}\text{Ir}$  brachytherapy standards for reference air kerma rate of the VSL and the BIPM *Metrologia* **51** Tech. Suppl. 06022
- Alvarez J T, Sander T, de Pooter J A, Allisy-Roberts P J and Kessler C 2014b Comparison BIPM.RI(I)-K8 of high dose rate  $^{192}\text{Ir}$  brachytherapy standards for reference air kerma rate of the NPL and the BIPM *Metrologia* **51** Tech. Suppl. 06024
- Bé M-M, Browne E, Chechev V, Helmer R and Schönfeld E 1999 Table of Radionuclides (Volume 5), CEA/Saclay – DIMRI/LNHB, F-91191 Gif-sur-Yvette, Cedex, France
- Behrens R and Pojtinger S 2023 PTB website [Scientific news from Division 6, 2023-08-15](#)
- Büermann L 2018 Changes to the magnitude of the unit of Gray according to ICRU Report 90: [https://www.ptb.de/cms/fileadmin/internet/fachabteilungen/abteilung\\_6/6.2/6.25/PTB\\_Information\\_ICRU90\\_Changes\\_to\\_Air\\_Kerma\\_25-Jan-2018.pdf](https://www.ptb.de/cms/fileadmin/internet/fachabteilungen/abteilung_6/6.2/6.25/PTB_Information_ICRU90_Changes_to_Air_Kerma_25-Jan-2018.pdf)
- CIPM MRA 1999 Mutual recognition of national measurement standards and of calibration and measurement certificates issued by national metrology institutes, International Committee for Weights and Measures (<https://www.bipm.org/en/cipm-mra/cipm-mra-documents>)
- ICRU 2016 Key data for ionizing-radiation dosimetry: Measurement standards and applications *J. ICRU* **14** Report 90 (Oxford University Press)
- Kessler C, Allisy-Roberts P J and Selbach H-J 2015 Comparison BIPM.RI(I)-K8 of high dose rate  $^{192}\text{Ir}$  brachytherapy standards for reference air kerma rate of the PTB and the BIPM *Metrologia* **52** Tech. Suppl. 06005
- Kessler C, Downton B and Mainegra-Hing E 2014 Comparison BIPM.RI(I)-K8 of high dose rate  $^{192}\text{Ir}$  brachytherapy standards for reference air kerma rate of the NRC and the BIPM *Metrologia* **52** Tech. Suppl. 06013
- KCDB 2023 The BIPM key comparison database (<https://www.bipm.org/kcdb>)
- Mainegra-Hing E and Rogers D 2006 On the accuracy of techniques for obtaining the calibration coefficient  $N_K$  of  $^{192}\text{Ir}$  HDR brachytherapy sources *Med. Phys.* **33**, 3340-3347.
- Pojtinger S and Büermann L 2021 Characterization of new primary air kerma standards for dosimetry in Co-60, Cs-137 and Ir-192 gamma ray sources *Journal of Instrumentation JINST* **16** P10014
- PTB website 2023 <https://www.ptb.de/cms/en/ptb/fachabteilungen/abt6/fb-62/625-dosimetry-for-diagnostic-radiology/primary-standards.html>
- PTW catalogue 2023 <https://www.ptwdosimetry.com/en/learning/online-catalog>

Selbach H-J and Büermann L 2004 Vergleich zweier Verfahren zur Darstellung der Einheit der Kenndosisleistung für  $^{192}\text{Ir}$ -HDR-Brachytherapiequellen in *Medizinische Physik 2004 – Tagungsband der 35. Jahrestagung der DGMP (Deutsche Gesellschaft für Medizinische Physik, Leipzig, 2004)* p. 82 ISBN 3-925218-84-X